The solid phases of deuterium sulphide by powder neutron diffraction

Jeremy K. Cockcroft

Institut Laue Langevin, B. P. 156X, 38042 Grenoble Cedex, France
and Max-Planck-Institut für Festkörperforschung, D-7000 Stuttgart 80,
Federal Republic of Germany

and Andrew N. Fitch

Department of Chemistry, University of Keele, Staffordshire ST5 5BG, U

Abstract. Powder neutron diffraction studies confirm that D_2S has 3 solid-state phases at ambient pressure. Phases I and II are cubic and orientationally disordered with space groups $Fm3m$ ($a = 5.8486(8)$ Å at 160 K) and $Pa3$ ($a = 5.7647(6)$ Å at 120 K), respectively. The deuterium scattering density arising from the disorder is modelled using symmetry-adapted spherical harmonic functions, which show a reduction from "twelve-fold" to "six-fold" disorder on cooling from phase I to phase II. For the fully ordered low-temperature phase III, a new structure has been determined which bears little resemblance to that reported in a previous neutron diffraction study. The structure is orthorhombic, space group $Pbcm$, with $a = 4.0760(1)$ Å, $b = 13.3801(5)$ Å and $c = 6.7215(3)$ Å at 1.5 K. The structure is essentially hexagonally close-packed, with distortions to accommodate the hydrogen atoms. The structure is antiferroelectric with the alignment of the molecular dipoles along the **a** direction.

Introduction

Deuterium sulphide solidifies below 187.1 K and has at least three solid phases between the melting point and liquid nitrogen temperature. Phase

---

Address for correspondence: Dr. Jeremy K. Cockcroft, Institut Laue Langevin, B. P. 156X, 38042 Grenoble Cedex, France.

transitions were reported at 132.8 K and 107.8 K from specific heat mea-
surements (Kruis and Clusius, 1937). This behaviour closely follows that
of hydrogen sulphide which melts at 187.6 K with equivalent transitions at
126.2 K and 103.5 K. The phase diagram of H_2S as a function of tempera-
ture and pressure has been determined by Stewart (1960). The nature of
the phases and the phase transitions have been investigated by a large
number of experimental methods, including dielectric constant measure-
ments (Havriliak, Swenson and Cole, 1955), infrared spectroscopy
(Anderson and Walmsley, 1965; Taimsalu and Robinson, 1965), NMR
(Look, Lowe and Northby, 1966; Collins, Ratcliffe and Ripmeester, 1989),
and Raman spectroscopy (Miller and Leroi, 1968; Anderson, Binbrek and
Tang, 1977; Anderson, Demoor and Hanson, 1987). The dielectric and
thermal measurements indicate that the orientations of the H_2S molecules
are ordered in the lowest-temperature phase, but disordered in the interme-
diate and high-temperature phases. The molecular structure was obtained
from microwave spectroscopy, and gave bond lengths of 1.3518 and
1.3474 Å and angles of 92.13° and 92.11° for H_2S and D_2S respectively
(Cook, De Lucia and Helminger, 1975).

Structural investigation of the solid has involved X-ray diffraction,
electron diffraction (Kitamura, Kashiwase, Harada and Honjo, 1961;
Harada and Kitamura, 1964), and powder neutron diffraction (Sándor and
Ogunade, 1969). From their X-ray and electron diffraction measurements
Harada and Kitamura (1964) reported that the lowest temperature phase
of H_2S is tetragonal, $a = 13.5$ Å, $c = 4.14$ Å, with $Z = 16$. This phase
transformed into the intermediate phase II via a transient phase, which was
also reported to be tetragonal, $a = 6.75$ Å, $c = 4.14$ Å, with $Z = 4$. The
presence of this transient phase was distinguished in the electron diffraction
pattern by the absence of weak odd-order reflections. From Patterson maps,
and from comparison of the observed and calculated electron diffraction
intensities, an arrangement of sulphur atoms was deduced for the transient
phase in the most probable space group $P4_2$. An equivalent arrangement
for the sulphur atoms in the stable lowest-temperature phase was then
proposed. The intermediate and high-temperature phases were reported as
face-centred cubic. The lattice parameter of the intermediate phase, $a =$
5.74 Å, increases sharply at the transition at 132.8 K to 5.78 Å, an increase
in volume of around 2% for the high-temperature phase.

From powder X-ray diffraction studies on H_2S and D_2S, and from
neutron diffraction studies on D_2S, Sándor and Ogunade (1969) have
reported more detailed structures including deuterium positions. At 102 K
the powder neutron diffraction pattern was indexed as tetragonal, $a =$
13.470(5) Å, $c = 4.101(4)$ Å. The structure was refined in space group $P4_2$,
$Z = 16$, from the integrated intensities of 18 composite peaks in the diffrac-
tion pattern. In the refinement the eleven independent sulphur positional
parameters were constrained to just one parameter, the twenty four deu-

terium positional parameters were constrained to five parameters, so that the eight independent S — D bond distances were reduced to two. For the intermediate phase, the appearance of additional peaks in the pattern following the transition from the f.c.c. phase I showed the structure to be primitive cubic, with $a = 5.739$ Å at 112 K. The structure was refined in space group $Pa\overline{3}$ from the intensities of eleven diffraction peaks, using a model which allows six-fold disorder of the D_2S molecules. In the high-temperature face-centred cubic phase it was assumed that there was substantial orientational disorder of the D_2S molecules.

Given the great improvements in flux and resolution of neutron powder diffractometers since the earlier studies, and the ability to refine complex crystal structures from good quality powder diffraction data using the Rietveld (1969) method, we felt that a more accurate determination of the solid state structures of an important molecule such as D_2S was appropriate. For orientationally disordered phases, it is possible to characterize the scattering density by use of symmetry-adapted spherical-harmonic (SASH) functions, whose coefficients can be refined from the neutron diffraction data, as was done for the high-temperature solid phases of SF_6 (Cockcroft and Fitch, 1988) and DBr (Cockcroft, Simon and Ziebeck, 1988a). Three phases are identified for D_2S, in agreement with the earlier experimental work, and their structures have been refined from high-resolution powder neutron diffraction data. The two higher-temperature phases are orientationally disordered, and a new orthorhombic structure is determined for the low-temperature phase, where the structure has been solved ab-initio from the powder diffraction data.

Theory

In a neutron diffraction experiment, the scattering density arising from a strongly librating or orientationally-disordered molecular species undergoing hindered rotations is often inadequately described by conventional positional and thermal parameters. Where the motion of the atoms is confined to the surface of a sphere, then the scattering density is most conveniently described in terms of symmetry-adapted spherical-harmonic (SASH) functions $K_{lm}(\theta,\phi)$ (Atoji and Lipscomb, 1954; Press and Hüller, 1973). In summary, the intensities of the Bragg reflections measured in a neutron diffraction experiment may be described by the equation

$$F_{hkl} = \sum_j F_j^{\text{rot}}(\mathbf{Q}) \exp(i\mathbf{Q} \cdot \mathbf{R}_j) \exp[-W_j(\mathbf{Q})]$$

with

$$F_j^{\text{rot}}(\mathbf{Q}) = 4\pi \sum_{l=0}^{\infty} \sum_{m=1}^{\infty} i^l j_l(Q\varrho) a_{lm} K_{lm}(\theta_Q, \phi_Q)$$

where F_{hkl} is the structure factor of the hkl^{th} reflection, $\mathbf{R}_j$ is the position of the jth shell of atoms with radius ϱ_j, $W_j(\mathbf{Q})$ is the translational Debye-Waller factor of the jth shell, and a_{lm} are the refinable coefficients which determine the scattering density within the jth shell. Examples of its application, particularly with reference to molecular structures with the space groups $Fm\bar{3}m$ and $Pa\bar{3}$, may be found in the papers by Press (1973), Cockcroft and Fitch (1988), Cockcroft et al. (1988a). A list of SASH functions which transform according to C_{3i} ($\bar{3}$) symmetry is given in the Appendix.

Experimental

D_2S was prepared by the reaction of ~ 20 g of CaS (Alfa, $>99\%$ pure) with a saturated solution of $MgCl_2 \cdot 6D_2O$ (300 g) in D_2O (Bickford, Wilkinson, Caley and Elving, 1939). Gaseous D_2S gently evolved on warming the mixture to $\sim 60°C$ and was collected in a liquid nitrogen cold trap. The cold trap containing the solid D_2S was transferred to a vacuum line and the D_2S was doubly distilled in vacuo into a silica-glass ampoule (length 7 cm by 12 mm internal $\varnothing$). After sealing, the sample was quickly transferred to a standard ILL orange cryostat precooled to 4 K.

Diffraction patterns of D_2S at 4 K were collected with $\lambda = 2.52$ Å on the high-flux multidetector diffractometer D1B at the Institut Laue Langevin, Grenoble, at several sample orientation angles in order to check the quality of the powder sample. No texture effects were apparent. Diffraction patterns were then obtained as a function of sample temperature over the range 1.5 K to 150 K. The rate of heating was $1°C/min$ up to 80 K, then $0.25°C/min$ from 80 K to 150 K. Diffraction patterns were stored every 2 min.

The sample was transferred to the high-resolution diffractometer D1A at the ILL and diffraction patterns were collected with $\lambda = 1.9106(1)$ Å (Ni calibration) at 1.5, 120, and 160 K over the 2θ-range 6° to 156° in steps of 0.05°. In addition, a pattern was obtained of D_2S at 1.5 K with $\lambda = 2.99$ Å over the same 2θ-range.

Results

The D1B diffraction data (Fig. 1) revealed two phase transitions for D_2S at approximately 109 K and 134 K (on heating) in agreement with specific heat (Kruis and Clusius, 1937) and earlier neutron diffraction measurements (Sándor and Ogunade, 1969). (The higher transition temperature is difficult to determine precisely as the only change in the diffraction pattern is the loss of intensity of the primitive cubic reflections.) The transient phase observed by electron diffraction between phases III and II (Harada and Kitamura, 1964) was not apparent.
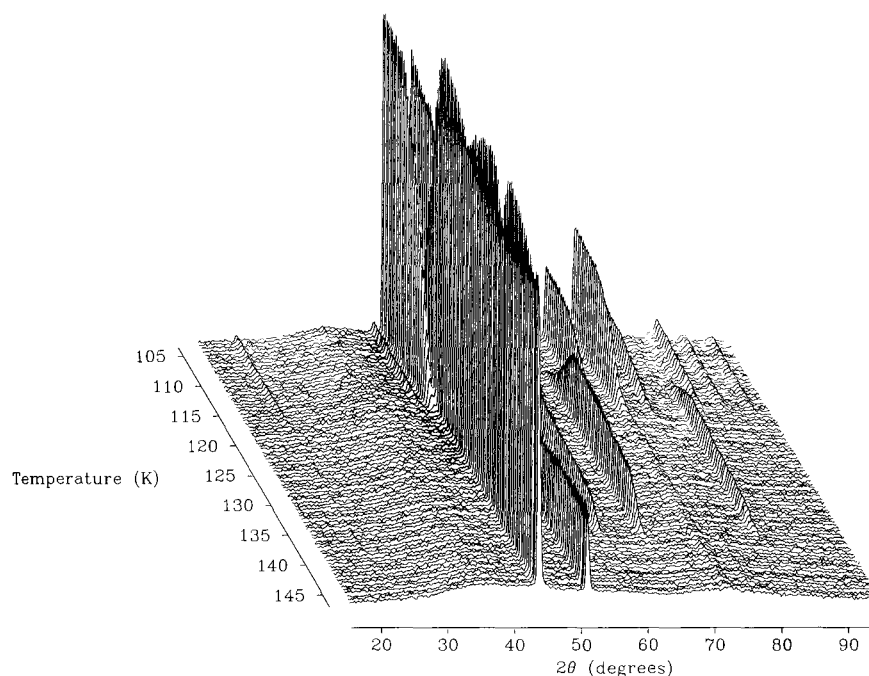
Fig. 1. Diffraction patterns of D$_2$S as a function of temperature obtained on D1B showing the I−II and II−III phase transitions.

The two high-temperature phases clearly correspond to the face-centred and primitive cubic phases reported previously by Sándor and Ogunade (1969). Although the peaks of the lowest-temperature phase could be indexed using their enlarged tetragonal cell, the intensities were very different from those calculated from their structural model. A closer examination of the model revealed internal inconsistencies. In particular, the fractional coordinates quoted do not produce the stated bond lengths and angles for the D$_2$S molecule. It proved impossible to find even typographical errors that could lead to chemically-reasonable values. Following the solution of the structure of the low temperature phase from the high-resolution neutron diffraction data (see below), the lattice parameters of all three phases were determined as a function of sample temperature, and are plotted in Figure 2.

From the 2.99 Å data set obtained on D1A, the 2θ-positions of 20 peaks were extracted and used as input to the automatic indexing program FZON by Visser (1969). The only solution produced which indexed all 20 lines and had a high figure-of-merit was a primitive orthorhombic cell. From the systematic absences the space group $Pbcm$ was indicated with lattice parameters $a = 4.079$ Å, $b = 13.421$ Å and $c = 6.728$ Å. The ratio $b/2c$, equal to 0.997, is close to unity and explains the observation of a tetragonal unit
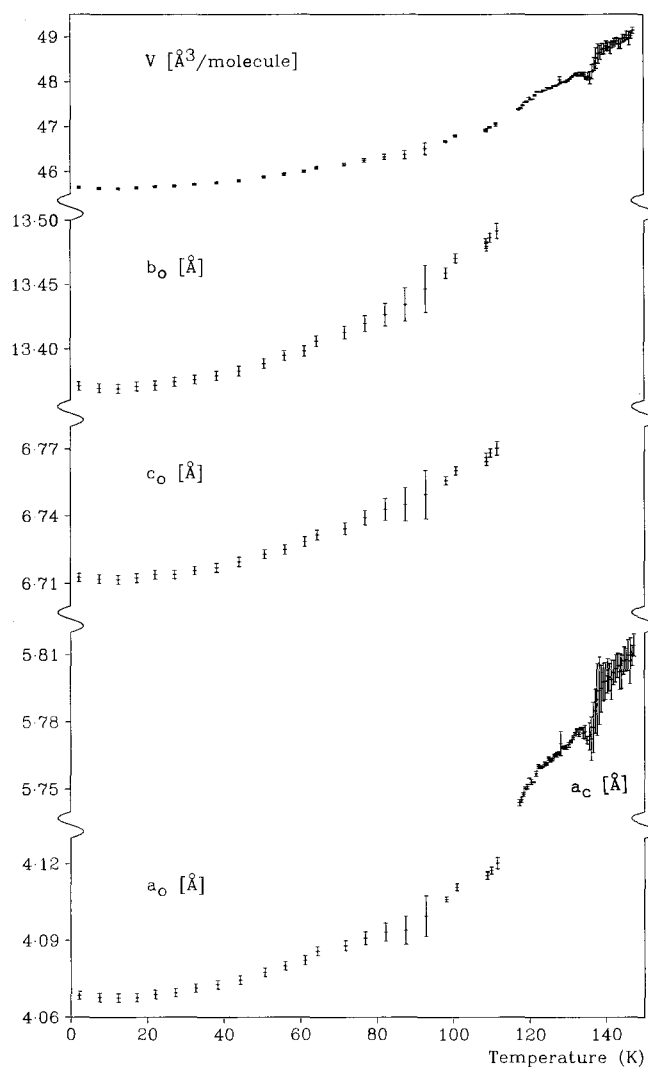
Fig. 2. Lattice parameters and volume per D_2S molecule as a function of temperature obtained from D1B data.

cell in the earlier neutron diffraction studies. The solution is also consistent with previous X-ray data which observed only the sulphur sublattice and had $a = b = 6.74$ Å and $c = 4.10$ Å.

Assuming that the sulphur positions approximately form a face-centred lattice (as indicated from the earlier X-ray and electron-diffraction studies) and that the deuterium atoms attempt to align in the direction of the nearest
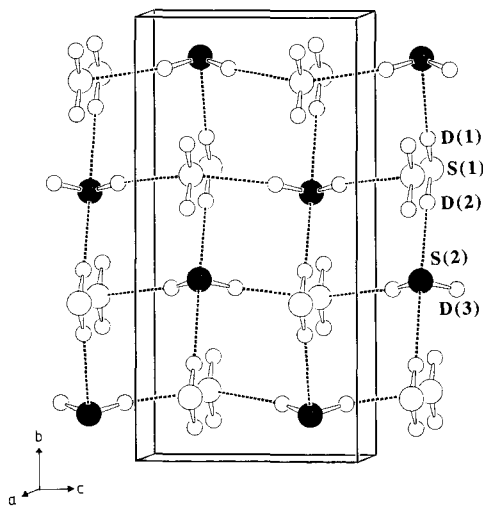
Fig. 3. SCHAKAL plot (Keller, 1989) of the structure of D_2S (III) seen along the a axis. Sulphur and hydrogen atoms are shown with large and small circles, respectively. Shaded S(2) atoms are close to the plane $x = 0.5$ whilst the unshaded S(1) atoms are close to the planes $x = 0$ and $x = 1$. Dotted lines show the nearest S − D...S interactions.

sulphur atoms, then there are few possibilities for the low-temperature structure. Attempts to order the D_2S molecules so that they all lie within a plane as in the hydrogen halides (Cockcroft et al., 1988; Cockcroft, Simon, Borrmann and Obermeyer, 1988) always fail to double the simple X-ray cell along only the b-direction. The only ordering scheme which both doubled the unit cell along b and which had the optimum D...S interactions is shown in Figure 3.

The structure was refined to a weighted profile R-factor of 10.0% in space group $Pbcm$ using the 1.9106 Å data. Neutron scattering lengths ($b_S = 2.847$ fm, $b_D = 6.674$ fm) were taken from the tables by Koester and Rauch (1983). The best fit to the data is shown in Figure 4 and the refined parameters are listed in Table 1. A total of 35 parameters were refined from 211 contributing reflections. The R-factor is slightly higher than that usually obtained on D1A and a closer comparison of the data sets obtained with $\lambda = 1.9106$ and 2.99 Å showed evidence of slight texture effects. In retrospect, these effects might have been reduced to an insignificant level by rotation of the sample during the course of the data acquisition. Rietveld refinements in lower symmetry space groups, e.g. $Pbc2_1$, did not significantly improve the fit to the data. Refinement of the deuterium site occupancy indicated that the deuterium level was better than 98%.

The highest-temperature phase of D_2S is face-centred cubic, space group $Fm\bar{3}m$, in common with many orientationally-disordered molecular struc-
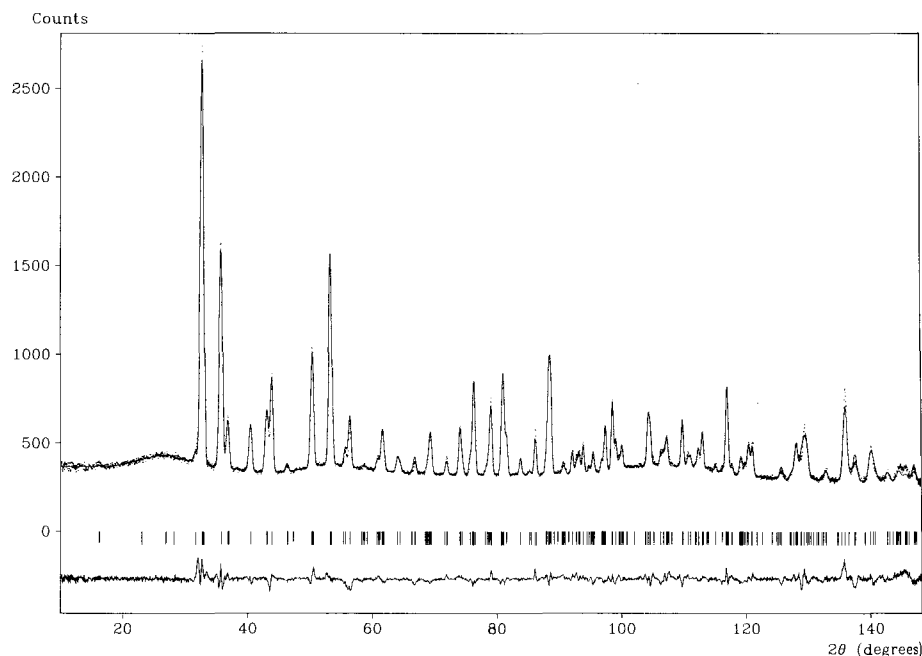
Counts

Fig. 4. Observed, calculated, and difference diffraction patterns for D_2S (III) at 1.5 K with $\lambda = 1.9106$ Å obtained on D1A at ILL, Grenoble. Vertical bars indicate calculated reflection positions.

tures (Fig. 5). From the 2θ-positions of 9 reflections, the lattice parameter refined to $a = 5.8486(8)$ Å. Graphical estimation of the background followed by profile summation yielded the intensities of 12 individual peaks. The structure was refined assuming that the sulphur atoms lie on the face-centred positions $(4a:0,0,0)$ and that the deuterium atoms form a spherical shell around each sulphur. There are only 3 SASH functions, K_{lm} (θ, ϕ), with O_h $(m\overline{3}m)$ point symmetry for $l \leq 6$ (Prandl, 1981). Least-squares refinement based on integrated peak intensities resulted in a weighted R-factor of 1.9% with an expected value of 1.1%. Inclusion of the next term, K_{81} (θ, ϕ), in the description of the deuterium density function did not significantly improve the fit. From the refined parameters, listed in Table 2, the calculated profile shown in Figure 5 was obtained. Observed and calculated peak intensities are given in Table 3. From the refined coefficients, a_{lm}, a stereographic projection of the deuterium scattering-density function was calculated and is shown in Figure 6.

The diffraction pattern of the intermediate phase II of D_2S differs from that of phase I by the presence of the non-face-centred cubic reflections,

Table 1. Final parameters, distances and angles for D$_2$S phase III refined from D1A data at a wavelength of 1.9106 Å. R-factors are defined as follows: $R_{wp} = \{\Sigma w[y(\text{obs}) - y(\text{calc})]^2/\Sigma wy(\text{obs})^2\}^{1/2} \times 100\%$, $R_{exp} = \{(N - P + C)/\Sigma wy(\text{obs})^2\}^{1/2} \times 100\%$, and $R_I = \{\Sigma |I(\text{obs}) - I(\text{calc})|/\Sigma I(\text{obs})\} \times 100\%$, where $w = 1/\sigma y(\text{obs})^2$. D$_2$S (III) at 1.5 K, space group *Pbcm* (No. 57), $Z = 8$; Cell constants a,b,c (Å): 4.0760(1), 13.3801(5), 6.7215(3); Volume per D$_2$S molecule: 45.822(4) Å^3; Calculated density: 1.307 g/cm^3; Peak-width parameters U,V,W ($^{\circ 2}$): 0.22(1), $-0.54(2)$, 0.49(1).

Atom	Site symmetry	X	Y	Z	B (Å^2)	N
S(1)	4*d m*	$-0.042(1)$	0.1449(5)	1/4	0.14(7)	4
S(2)	4*d m*	0.460(0)	0.4017(5)	1/4	0.14(7)	4
D(1)	4*d m*	0.173(1)	0.2168(3)	1/4	3.7[a]	4
D(2)	4*d m*	0.194(1)	0.0736(3)	1/4	3.6[a]	4
D(3)	8*e* 1	0.6724(7)	0.3797(2)	0.1057(4)	2.9[a]	8

Atom	B [1,1] (Å^2)	B [2,2]	B [3,3]	B [1,2]	B [2,3]	B [3,1]
D(1)	3.5(2)	2.8(2)	4.7(3)	$-1.2(2)$	0	0
D(2)	2.4(3)	4.2(2)	4.1(3)	2.2(2)	0	0
D(3)	2.1(1)	3.0(1)	3.4(2)	0.7(1)	$-0.2(1)$	1.6(1)

R-factors: $R_{wp} = 10.1\%$, $R_{exp} = 5.1\%$, $R_I = 7.4$.

[a] Equivalent isotropic B-values calculated from refined anisotropic B-values.

Distances (Å) and angles ($^\circ$)

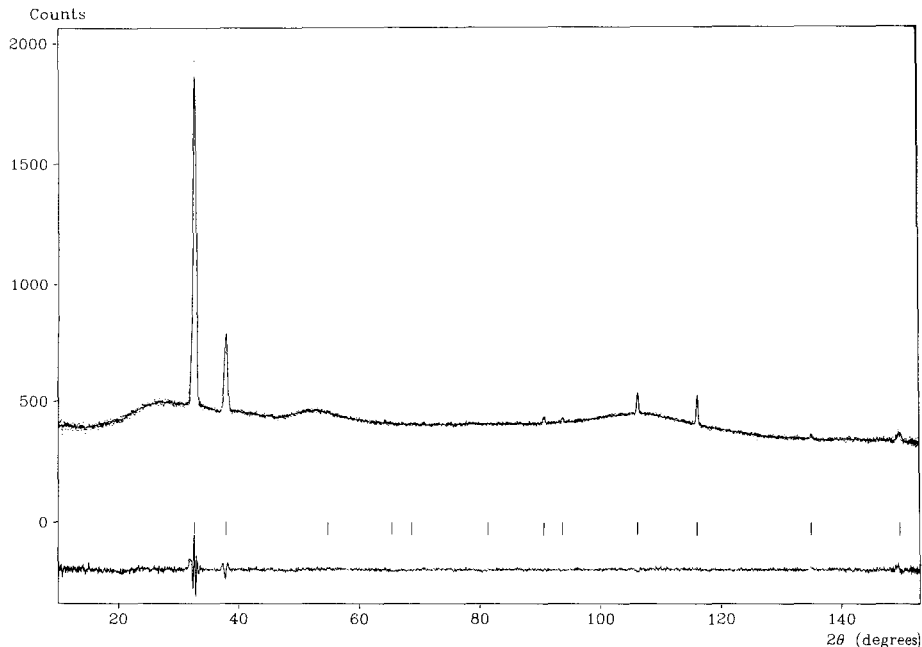|				
1 × S(1) − D(1)	1.301(8)		1 × D(1) − S(1) − D(2)	92.4(4)
1 × S(1) − D(2)	1.354(8)			
2 × S(2) − D(3)	1.332(8)		1 × D(3) − S(2) − D(3)	93.4(4)
2 × S(1)...D(3)	2.680(4)		1 × D(3)...S(1)...D(3)	126.4(2)
1 × S(2)...D(1)	2.738(4)		1 × D(1)...S(2)...D(2)	173.8(3)
1 × S(2)...D(2)	2.699(4)			
			2 × S(1)...D(3) − S(2)	163.4(3)
			1 × S(1) − D(1)...S(2)	163.0(4)
			1 × S(1) − D(2)...S(2)	166.3(4)
2 × S(1)...S(1)	4.076(8), 4.382(6)			
1 × S(1)...S(2)	3.672(9), 3.990(9)			
1 × S(1) − D(1)...S(2)	4.001(9)			
1 × S(1) − D(2)...S(2)	4.027(9)			
2 × S(1)...S(2)	3.974(5)			
2 × S(1)...D(3) − S(2)	3.985(5)			
2 × S(2)...S(2)	4.076(9), 4.280(6)			

Fig. 5. Diffraction pattern of D_2S (I) at 160 K. The calculated pattern is obtained from the structural parameters refined from the integrated peak intensity data with the instrumental parameters (a, U,V,W, zp, and scale) refined from the pattern. Vertical bars indicate calculated reflection positions.

Table 2. Final parameters for D_2S phase I. R-factors are defined as follows: $R_{12} = \{\Sigma w[I(\text{obs}) - I(\text{calc})]^2/\Sigma wI(\text{obs})^2\}^{1/2} \times 100\%$ and $R_{\text{exp}} = \{(N - P + C)/\Sigma wI(\text{obs})^2\}^{1/2} \times 100\%$, where $w = 1/\sigma I(\text{obs})^2$. D_2S (I) at 160 K, space group $Fm\bar{3}m$ (No. 225), $Z = 4$; Cell constant $a(\text{Å})$: 5.8486(8); Volume per D_2S molecule: 50.01(2) Å^3; Calculated density: 1.195 g/cm^3.

Atom	Site symmetry	X	Y	Z	$B(\text{Å}^2)$	N
S	$4a\ m\bar{3}m$	0	0	0	6.5(6)	4
D shell	$4a\ m\bar{3}m$	0	0	0	5.7(8)	8

D shell parameters: $r_{\text{S}-\text{D}} = 1.28(2)$ Å, $a_{01} = b_D/\sqrt{(4\pi)}$ fm, $a_{41} = -0.32(1)$ fm, $a_{61} = -0.77(2)$ fm. R-factors: $R_{12} = 1.9\%$, $R_{\text{exp}} = 1.1\%$.

Figure 7. The absence of the 100 and 110 reflections immediately suggests the space group $Pa\bar{3}$ (a direct subgroup of $Fm\bar{3}m$) for D_2S (II). The lattice parameter was determined from the peak positions of 17 reflections as $a = 5.7647(6)$ Å. Profile integration similar to that used for phase I yielded the intensities of 26 peaks. Assuming that the transition from phase I to phase II

Table 3. Observed and calculated intensities for D_2S phase I.

H	K	L	J	I(obs)	I(calc)	ΔI	σI(obs)	$\Delta I/\sigma I$
1	1	1	8	18275	18260	15	84	0.2
2	0	0	6	4075	4113	−38	64	0.6
2	2	0	12	109	20	89	43	2.1
3	1	1	24	0	27	−27	38	0.7
2	2	2	8	46	48	−2	38	0.1
4	0	0	6	0	3	−3	38	0.1
3	3	1	24	237	257	−20	41	0.5
4	2	0	24	151	149	2	39	0.1
4	2	2	24	594	658	−64	41	1.6
3	3	3	8 ⎫	933	870	63	44	1.4
5	1	1	24 ⎭					
4	4	0	12	207	71	136	45	3.0
5	3	1	48	516	550	−34	57	0.6
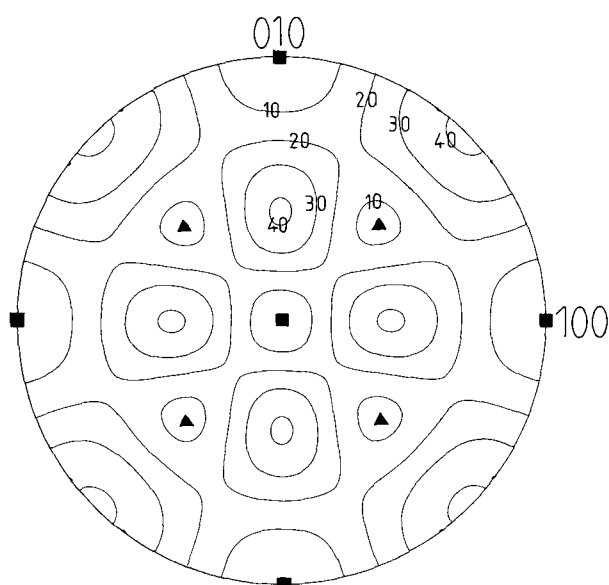
Fig. 6. Stereographic projection viewed down the z-axis of the deuterium scattering density of the disordered D_2S phase I. The maxima and minima of the density function correspond to the $\langle 110 \rangle$ and $\langle 111 \rangle$, $\langle 100 \rangle$ directions, respectively.

involves only changes in the deuterium disorder, then the sulphur atoms still form a face-centred lattice and are sited on the position $4a:0,0,0$ in space group $Pa3$. If the deuterium atoms are still significantly disordered around the sulphur, then they will form a shell as in phase I, but with the lower point symmetry of C_{3i} ($\bar{3}$).
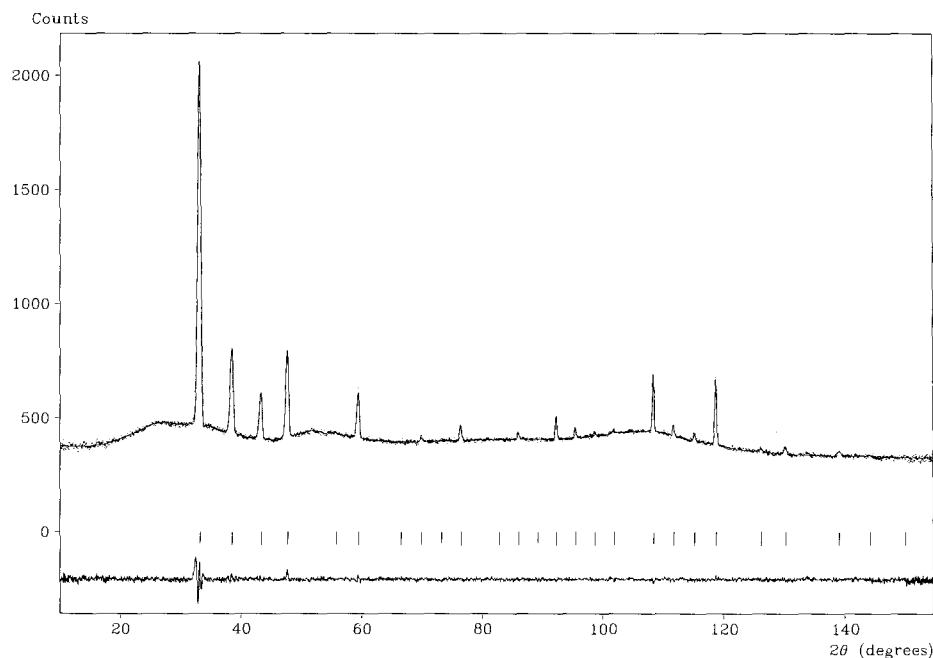
Fig. 7. Diffraction pattern of D_2S II at 120 K. Calculated pattern obtained as for Figure 4.

There are 10 SASH functions for $l \le 6$ with C_{3i} ($\bar{3}$) symmetry (Prandl, 1981; see Appendix). Refinement of the structure using these 10 SASH functions to describe the deuterium scattering density gave an excellent fit to the data with an integrated intensity R-factor of 1.7%, expected 1.7%, the observed and calculated intensities being listed in Table 4. From the refined values of the coefficients a_{lm} given in Table 5, the stereographic projection shown in Figure 8 was calculated. The refinement posed two problems: As with HBr (Ib) (Cockcroft et al., 1988a), the sign of the coefficients a_{lm} which do not have O_h ($m3m$) symmetry may be inverted to give a different density function but an identical fit to the observed intensities. However, the alternative model had a sufficiently non-positive definite density function for it to be rejected. Secondly, with the limited number of observations available, the coefficient a_{62} is determined solely from one peak intensity to which it has virtually no contribution. Its value, which must be small, was set arbitrarily to zero to improve the stability of the refinement.

In both refinements of phases I and II of D_2S, the isotropic B-factor for S and D were left unconstrained so as to allow for the possibility that the S atom could be slightly displaced from 0,0,0. This would result in a

Table 4. Observed and calculated intensities for D_2S phase II.   **13**

H	K	L	J	I(obs)	I(calc)	ΔI	σI(obs)	ΔI/σI
1	1	1	8	20785	20788	−3	107	0.0
2	0	0	6	4673	4663	10	81	0.1
2	1	0	12	2456	2448	8	71	0.1
2	1	1	24	4461	4433	28	74	0.4
2	2	0	12	136	122	14	57	0.2
2	2	1	24	2035	2095	−60	64	0.9
3	1	1	24	102	15	87	54	1.6
2	2	2	8	214	193	21	55	0.4
3	0	2	12	0	106	−106	55	1.9
3	1	2	24 ⎫	600	583	17	60	0.3
3	2	1	24 ⎭					
4	0	0	6	51	3	48	56	0.9
4	1	0	12 ⎫	214	243	−29	53	0.5
3	2	2	24 ⎭					
4	1	1	24	0	3	−3	53	0.1
3	3	1	24	803	757	46	54	0.9
4	0	2	12 ⎫	317	326	−9	52	0.2
4	2	0	12 ⎭					
4	1	2	24 ⎫	163	134	29	46	0.6
4	2	1	24 ⎭					
3	3	2	24	184	131	53	47	1.1
4	2	2	24	1620	1698	−78	56	1.4
4	3	0	12	358	341	17	53	0.3
4	1	3	24 ⎫	267	268	−1	51	0.0
4	3	1	24 ⎭					
5	1	1	24 ⎫	2266	2226	40	56	0.7
3	3	3	8 ⎭					
4	3	2	24 ⎫	146	161	−15	51	0.3
4	2	3	24 ⎬					
5	0	2	12 ⎭					
5	2	1	24 ⎫	380	373	7	52	0.1
5	1	2	24 ⎭					
4	4	0	12	361	364	−3	57	0.1
5	2	2	24 ⎫	177	133	44	59	0.7
4	4	1	24 ⎭					
4	3	3	24	75	109	−34	71	0.5

Table 5. Final parameters for D_2S phase II. R-factors defined as in Table 2. D_2S (II) at 120 K, space group $Pa\bar{3}$ (No. 205), $Z = 4$; Cell constant $a(\text{Å})$: 5.7647(6); Volume per D_2S molecule: 47.89(1) Å^3; Calculated density: 1.248 g/cm^3.

Atom	Site symmetry	X	Y	Z	$B(\text{Å}^2)$	N
S	$4a\,\bar{3}$	0	0	0	3.2(2)	4
D shell	$4a\,\bar{3}$	0	0	0	3.7(3)	8

D shell parameters: $r_{D-D} = 1.25(1)$ Å; $a_{01} = b_D/\sqrt{(4\pi)}$ fm; $a_{21} = -2.87(6)$ fm; $a_{41} = -0.57(6)$, $a_{42} = -0.39(7)$, $a_{43} = 1.90(8)$ fm; $a_{61} = -0.74(9)$, $a_{62} = 0$, $a_{63} = -1.16(30)$, $a_{64} = 0.07(24)$, $a_{65} = 0.42(23)$ fm; R-factors: $R_{I2} = 1.9\%$, $R_{exp} = 1.1\%$.
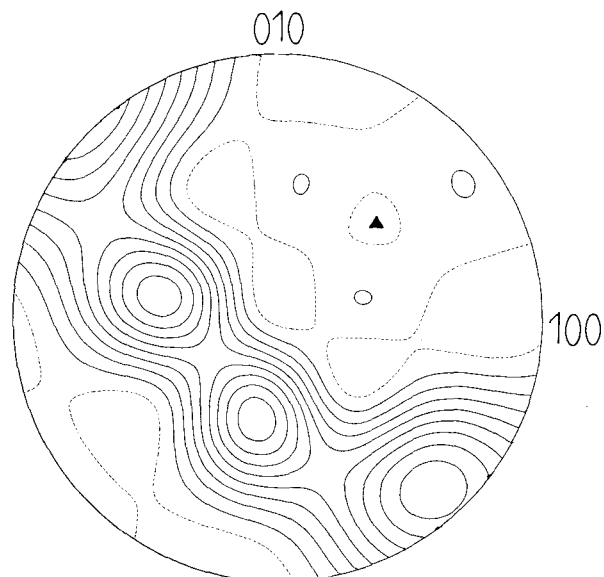
Fig. 8. Stereographic projection viewed down the z-axis of the deuterium scattering density of the disordered D_2S phase II. The deuterium are distributed on a torus whose axis lies along 111.

slightly higher B-factor for S than for D. However, within experimental error, there is little difference between the B-factors indicating that the position of the sulphur atom can be taken as the mean centre of gravity of the molecule.

Conclusion

The existence of three solid phases for D_2S has been confirmed, in agreement with earlier workers using a wide range of physical techniques. The occurrence of a transient phase between phases II and III, as seen in the electron microscope (Harada and Kitamura, 1964) could not be substantiated for the bulk material.

Phase I, which is face-centred cubic, and phase II, which is primitive cubic, both contain four molecules per unit cell and are orientationally disordered. There is a change in volume of around 2% on cooling through the transition at 132.8 K as the molecules pack together more closely in phase II. The average scattering density of the hydrogen atoms in these phases has been modelled in terms of symmetry-adapted spherical-harmonic functions which indicate that the degree of orientational disorder is

lower in phase II than in phase I, as would be expected. Stereographic projections of the disordered hydrogen density are shown in Figures 6 and 8. The density functions show that in the face-centred phase I the deuterium density is oriented with equal probability towards each of the twelve neighbouring D$_2$S molecules, whereas in the intermediate phase II the deuterium density is directed with equal probability towards only six neighbouring molecules within a close-packed layer. A very similar transition is observed for HBr between phases Ia and Ib (Cockcroft et al., 1988a).

For the lowest-temperature phase III, a new structure has been determined in the orthorhombic space group *Pbcm*, with eight molecules per unit cell, in contrast to earlier diffraction studies which suggested a tetragonal structure. Whilst the arrangement of the sulphur atoms is very close to tetragonal, there is little correspondence between the positions of the hydrogen atoms and those deduced from the neutron diffraction work of Sándor and Ogunade (1969). The latter's refinement was based upon eighteen composite integrated intensities over an angular range containing 184 individual reflections (389 reflections using their tetragonal model!). It is not surprising then that problems should have arisen in the refinement of their structure.

The structure of phase III of D$_2$S can be understood in terms of the influence of close packing of molecules and of dipole-dipole interactions. Shortening of sulphur-sulphur contact distances due to hydrogen bonding is not evident, and therefore it is likely that the hydrogen-sulphur dipoles play the dominant role in binding the structure together.

The structure is hexagonally close-packed, with distortions to accommodate the hydrogen atoms. The close-packed layers are at $z = 1/4$ and $z = 3/4$ and lie parallel with the (001) planes. Within the layers each sulphur has six neighbours, Figure 9, with three other neighbours in each of the layers immediately above and below, giving an overall co-ordination number of twelve.

Within the layers the molecules pack together one behind the other along the **a** direction, separated by |**a**| (4.0761 Å), with their dipoles roughly aligned. The dipoles of the molecules lie in the plane of the close-packed layer, and are oriented with respect to **a** at angles of 1.5 and 18.6 degrees for S(1) and S(2) respectively. Molecules for which $1/2 < y < 1$ have their dipoles along the positive **a** direction, whereas those for which $0 < y < 1/2$ have their dipoles along the negative **a** direction, thereby forming layers (of thickness |**b**|/2) perpendicular to **b** in which the molecules are all closely aligned. The c-glide planes at $y = 1/4$ and $y = 3/4$ together with the mirror planes perpendicular to **c** ensure that the resultant polarisation of each of these layers lies precisely along **a**, so that the overall polarisation per unit cell is zero. The structure is, therefore, antiferroelectric.

Within the close-packed layers, each S(1) has close contacts with two S(1) atoms (along **a**) and four S(2) atoms, and each S(2) with two S(2) atoms
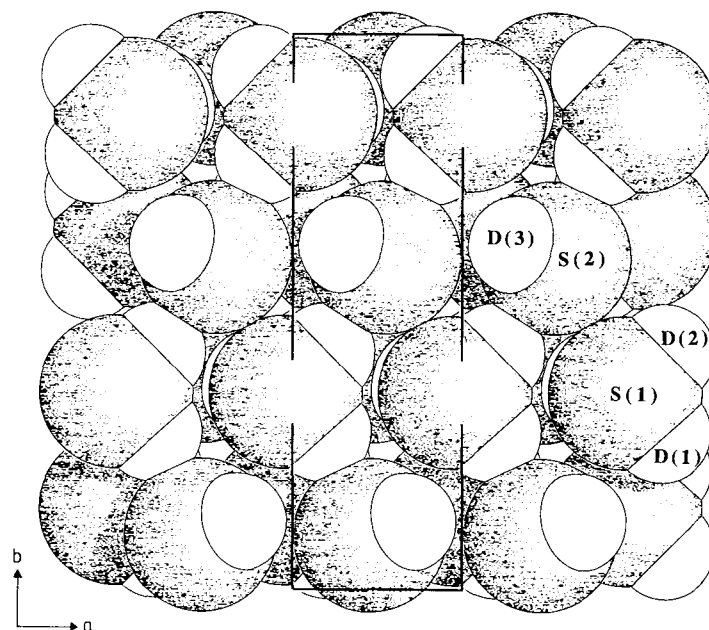
Fig. 9. Packing diagram of D_2S phase III viewed down the c-axis of the unit cell showing the close-packed molecules in the ab-plane [SCHAKAL plot, Keller (1989)].

(along **a**) and four S(1) atoms (Fig. 9). Of these four S(1)—S(2) contacts, two resemble hydrogen-bonded interactions via D(1) and D(2), with S(1)—S(2) distances of 4.001(9) Å and 4.027(9) Å, respectively. The third contact, which does not involve hydrogen directly, is 3.990(9) Å. The shortest S(1)—S(2) contact distance of 3.672(9) Å involves two molecules whose deuterium atoms point in nearly opposite directions. If the van-der-Waals radius of sulphur is taken as 1.85 Å (Pauling, 1970), then this is the minimum contact distance that could be expected between sulphur atoms. S(1)—S(2) contacts between successive close-packed layers involve another interaction that resembles a hydrogen-bond via D(3) (3.985(5) Å) which is slightly longer than the more direct interaction at 3.974(5) Å. The longest S—S interactions, ranging from 4.076(8) Å to 4.382(6) Å, correspond to the S(1)—S(1) and S(2)—S(2) distances between the close-packed layers.

In the structure there are what appear to be three hydrogen-bonded interactions, via D(1), D(2) and D(3) (Fig. 3). Table 1 summarises the relevant bond distances and angles. It is apparent that all three linkages have similar distances and angles. However, the S(1)—S(2) contacts are all considerably longer than the sum of the van-der-Waals radii, suggesting that such hydrogen bonding that may occur is weak, and that the packing

of the molecules is more dominant in determining the relevant sulphur—sulphur contacts. The geometry of S(1) is approximately tetrahedral, with internal angles ranging from the bond angle of $92.4(4)°$ to the angle of $126.4(2)°$ between the two D(3) atoms which link adjacent S(2) molecules above and below the ab-plane. The environment of S(2) is more distorted with $D-S-D$ angles ranging from $81.3(3)°$ to $173.8(3)°$ but with a normal internal angle for the D_2S molecule of $93.4(4)°$. The incoming D(1) and D(2) atoms linking to S(1) molecules within the close-packed layer are disposed at $173.8(3)°$ to each other. Further, the D(2) atom actually approaches the S(2) from the same side as the bonded D(3) atoms with a $D(2)-S(2)-D(3)$ angle of only $81.3(3)°$.

The $S-S$ and $S-D...S$ interactions in D_2S are similar to those of the SD^- ion in the low-temperature phase of CsSD (Jacobs and Kirchengässner, 1989) where the SD^- ions order in planes as in DI (Cockcroft et al., 1989). Within the SD^- layers in CsSD, the $S-D...S$ distance is larger than the $S...S$ distance [$4.041(4)$ Å versus $4.183(4)$ Å, respectively] showing that dipole—dipole interactions are more significant than hydrogen bonding. The near absence of hydrogen bonding in the solid state phases of D_2S should be reflected in the properties of liquid D_2S and indeed this is the case. Recent studies of liquid deuterium sulphide, measured on the LAD diffractometer at ISIS (Andreani, Merlo, Ricci, Ruocci and Soper, 1989), also demonstrated, perhaps not surprisingly, that hydrogen bonding is also absent in the liquid phase.

Appendix

Symmetry-adapted spherical-harmonic functions for $l \le 6$ which transform according to C_{3i} ($\bar{3}$) symmetry with the 3-fold axis along [111]. For the case of the 3-fold axis lying along [$\bar{1}\bar{1}1$], [$1\bar{1}\bar{1}$], or [$\bar{1}1\bar{1}$] (as found in space group $Pa\bar{3}$), the operand (x,y,z) should be multiplied by $(-1,-1,1)$, $(1,-1,-1)$, or $(-1,1,-1)$, respectively. Note that the value of m is assigned arbitrarily.

$K_{lm}(X,Y,Z)$	Symmetry
$K_{01}(X,Y,Z) = 1/\sqrt{(4\pi)}$	O_h
$K_{21}(X,Y,Z) = \sqrt{(15)} \, (XY + YZ + ZX)/3\sqrt{(4\pi)}$	C_{3i}
$K_{41}(X,Y,Z) = 5\sqrt{(21)} \, (X^4 + Y^4 + Z^4 - 3/5)/4\sqrt{(4\pi)}$	O_h
$K_{42}(X,Y,Z) = 3\sqrt{(35)} \, [XYX^2 - Y^2) + YZ(Y^2 - Z^2) + ZX(Z^2 - X^2)]/6\sqrt{(4\pi)}$	C_{3i}

$K_{lm}(X,Y,Z)$	Symmetry
$K_{43}(X,Y,Z) = 21\sqrt{(5)}\,[XY(Z^2 - 1/7)$ $+ YZ(X^2 - 1/7) + ZX(Y^2 - 1/7)]/6\sqrt{(4\pi)}$	C_{3i}
$K_{61}(X,Y,Z) = 231\sqrt{(26)}\,[(X^2Y^2Z^2 + X^4 + Y^4 + Z^4 - 3/5)/$ $22 - 1/105]/8\sqrt{(4\pi)}$	O_h
$K_{62}(X,Y,Z) = \sqrt{(30030)}\,[X^4(Y^2 - Z^2)$ $+ Y^4(Z^2 - X^2) + Z^4(X^2 - Y^2)]/8\sqrt{(4\pi)}$	C_{3i}
$K_{63}(X,Y,Z) = 33\sqrt{(91)}\,[XY(X^2 - Y^2)(Z^2 - 1/11)$ $+ YZ(Y^2 - Z^2)(X^2 - 1/11) + ZX(Z^2 - X^2)$ $(Y^2 - 1/11)]/12\sqrt{(4\pi)}$	C_{3i}
$K_{64}(X,Y,Z) = 33\sqrt{(2730)}\,[YZ(X^4 - 6X^2/11 + 1/33)$ $+ ZX(Y^4 - 6Y^2/11 + 1/33)$ $+ XY(Z^4 - 6Z^2/11 + 1/33)]/48\sqrt{(4\pi)}$	C_{3i}
$K_{65}(X,Y,Z) = \sqrt{(6006)}\,[XY(X^4 + Y^4 - 5(X^2 + Y^2)^2/8)$ $+ YZ(Y^4 + Z^4 - 5(Y^2 + Z^2)^2/8)$ $+ ZX(Z^4 + X^4 - 5(Z^2 + X^2)^2/8)]/6\sqrt{(4\pi)}$	C_{3i}

References

Anderson, A., Binbrek, O. S., Tang, H. C.: Raman and infrared study of the low temperature phase of solid H_2S and O_2S. J. Raman Spectrosc. **6** (1977) 213−220.

Anderson A., Demoor, S., Hanson, R. C.: Raman study of a new high pressure phase of hydrogen sulphide. Chem. Phys. Lett. **140** (1987) 471−475.

Anderson, A., Walmsley, S. H.: Far infra-red spectra of molecular crystals IV. ammonia, hydrogen sulphide and their fully deuterated analogues. Mol. Phys. **9** (1965) 1−8.

Andreani, C., Merlo, V., Ricci, M. A., Ruocco, G., Soper, A. K.: Structure factor for liquid deuterium sulphide. ISIS Annual report (RAL-88-050), Swindon Press Ltd., Experimental reports (1988) A65. Europhys. Lett. **8** (1989) 441−446.

Atoji, M., Lipscomb, W. N.: The X-ray scattering from a hindered rotator. III. Acta Crystallogr. **7** (1954) 726−729.

Bickford, W. D., Wilkinson, J. A., Caley, E. R., Elving, P. J.: Liquid hydrogen sulphide. Inorg. Synth. **1** (1939) 111−113.

Cockcroft, J. K., Fitch, A. N.: The solid phases of sulphur hexafluoride by powder neutron diffraction. Z. Kristallogr. **184** (1988) 123−145.

Cockcroft, J. K., Simon, A., Ziebeck, K. R. A.: The structures of crystalline hydrogen bromide. Z. Kristallogr. **184** (1988a) 229−246.

Cockcroft, J. K., Simon, A., Borrmann, H., Obermeyer, A.: The crystal structure of the low-temperature modifications of deuterium iodide − a neutron study. Eur. J. Solid State Inorg. Chem. **25** (1988b) 471−481.

Collins, M. J., Ratcliffe, C. I., Ripmeester, J. A.: ^2H and ^{33}S NMR line-shape studies of the molecular motion in the liquid and solid phases of hydrogen sulphide and solid phase II of hydrogen selenide. J. Phys. Chem. **93** (1989) 7495−7502.

Cook, R. L., De Lucia, F. C., Helminger, P.: Molecular force field and structure of hydrogen sulphide: recent microwave results. J. Mol. Struct. **28** (1975) 237—246.

Harada, J., Kitamura, N.: Structure and phase transition of solid hydrogen sulphide. J. Phys. Soc. Japan **19** (1964) 329—343.

Havriliak, S., Swenson, R. W., Cole, R. H.: Dielectric constants of liquid and solid hydrogen sulphide. J. Chem. Phys. **23** (1955) 134—135.

Jacobs, H., Kirchengässner, R.: Bindungsverhältnisse in kristallinen Phasen von Caesiumhydrogensulfid, CsSH und CsSD. Z. Anorg. Allg. Chem **569** (1989) 117—130.

Keller, E.: Some computer drawings of molecular and solid-state structures. J. Appl. Crystallogr. **22** (1989) 19—22.

Kitamura, N., Kashiwase, Y., Harada, J., Honjo, G.: Electron diffraction study of the phase transition of hydrogen sulphide at $-170°C$. Acta Crystallogr. **14** (1961) 687—688.

Koester, L., Rauch, H.: Recommended values of neutron scattering lengths. IAEA Rep. No. 2517/RB, International Atomic Energy Agency, Vienna (1983).

Kruis, A., Clusius, K.: Über die Molwärmen und Umwandlungen der kondensierten Hydride und Deuteride des Schwefels und Selens, Z. Phys. Chem. **B38** (1937) 156—176.

Look, D. C., Lowe, I. J., Northby, J. A.: Nuclear magnetic resonance study of molecular motions in solid hydrogen sulphide. J. Chem. Phys. **44** (1966) 3441—3452.

Miller, R. E., Leroi, G. E.: Raman spectra of polycrystalline H_2S and D_2S. J. Chem. Phys. **49** (1968) 2789—2797.

Pauling, L., *General Chemistry*, 3rd edn. W. H. Freeman & Co. San Francisco (1970) 197.

Prandl, W.: The structure factor of orientationally disordered crystals: the case of arbitrary space, site and molecular point group. Acta Crystallogr. **A37** (1981) 811—818.

Press, W.: Analysis of orientationally disordered structures. II. Examples. Solid CD_4, p-D_2 and ND_4Br. Acta Crystallogr. **A29** (1973) 257—263. *Erratum* Acta Crystallogr. **A32** (1976) 170.

Press, W., Hüller, A.: Analysis of orientationally disordered structures. I. Method. Acta Crystallogr. **A29** (1973) 252—256.

Rietveld, H. M.: A profile refinement method for nuclear and magnetic structures. J. Appl. Crystallogr. **2** (1969) 65—71.

Sándor, E., Ogunade, S. O.: Structure and phase transition in solid hydrogen and deuterium sulphides. Nature **224** (1969) 905—907.

Stewart, J. W.: Compression and phase transitions of solid NH_3, SiF_4, H_2S, and CF_4. J. Chem. Phys. **33** (1960) 128—133.

Taimsalu, P., Robinson, D. W.: The far-infrared spectra of solid H_2S and D_2S at 5 K and 77 K. Spectrochim. Acta **21** (1965) 1921—1926.

Visser, J. W.: A fully automatic program for finding the unit cell from powder data. J. Appl. Crystallogr. **2** (1969) 89—95.